Low pressure oxidation of ordered Sn/Pd(110) surface alloys

2009 J. Phys.: Condens. Matter 21 185011

(http://iopscience.iop.org/0953-8984/21/18/185011)

J. Phys.: Condens. Matter **21** (2009) 185011 (9pp) doi:10.1088/0953-8984/21/18/185011

Low pressure oxidation of ordered Sn/Pd(110) surface alloys

N Tsud[1,2,5], T Skála[3], F Šutara[1], K Veltruská[1], V Dudr[4], M Yoshitake[2], K C Prince[3] and V Matolín[1]

[1] Faculty of Mathematics and Physics, Department of Surface and Plasma Science, Charles University, V Holešovičkách 2, 18000 Prague 8, Czech Republic
[2] National Institute for Materials Science, 3-13, Sakura, Tsukuba 305-0003, Japan
[3] Sincrotrone Trieste, Strada Statale 14, km 163.5, 34012 Basovizza-Trieste, Italy
[4] Institute of Physics, Academy of Sciences of the Czech Republic, Cukrovarnická 10, 16253 Prague 6, Czech Republic

E-mail: tsud@mbox.troja.mff.cuni.cz

Received 21 October 2008, in final form 3 March 2009
Published 24 March 2009
Online at stacks.iop.org/JPhysCM/21/185011

Abstract
The reaction of oxygen at low pressure with the Sn/Pd(110) system has been examined by photoelectron spectroscopy using synchrotron radiation. The c(2 × 2) and (3 × 1) reconstructions of the Sn/Pd(110) surface at 0.5 and 0.7 monolayers (ML) Sn coverage and a 1.75 ML Sn overlayer on the Pd(110) surface after flashing to 470 K were studied. The Sn 4d core level is strongly affected by O_2 adsorption while the Pd 3d core level shows very little change other than a decrease in intensity. Starting with a 10 L dose of oxygen, prominent changes in the spectra were observed for all Sn/Pd(110) surface alloys. Analysis of the Sn 4d core levels indicates that oxidation proceeds with the formation of well-defined states of Sn, which were identified as a Pd–Sn–O interface layer, SnO and SnO_2 oxides. The valence band spectra confirm this assignment. The Sn^{2+} and Sn^{4+} component signals originate from the topmost surface layer, i.e. tin atoms in more highly oxidized states constitute the topmost surface layer on top of the Pd–Sn–O interface. The presence of a sub-surface PdSn intermetallic alloy facilitates the tin oxide formation; the Sn–O phase formation is accompanied by Pd–Sn bond dissociation.

(Some figures in this article are in colour only in the electronic version)

1. Introduction

Tin oxide is a promising material for development of advanced nanoelectronics devices, catalysts and sensors and the surface electronic properties are crucial for understanding the sensing and catalytic properties of tin-oxide-based materials [1, 2]. The identification of the oxidation states of the Sn atom for different SnO_x systems (powders, evaporated films, polycrystalline foils and bimetallic compounds of tin with transition metals) by surface-sensitive methods has been much discussed in the literature. Core level and valence band spectroscopy of SnO_x systems is a successful method for determining the extent of tin atom interaction with oxygen [3, 4].

Oxidation of Sn metal foils by O_2 exposures from 200 up to 8×10^{11} L at 300 K was studied by synchrotron radiation photoemission by De Padova *et al* [3]. It was shown that the oxidation of the tin foil surface in the first stage (200–10^6 L) gives predominantly SnO oxide, whereas at higher exposures it proceeds through the formation of SnO_2. It was concluded that the SnO_2 overlayer on an SnO interface film represents a common structure of the oxide film formed on the tin metal surface. No detectable change of the Sn 4d core levels after adsorption of 200 L of O_2 at 300 K was observed. For higher O_2 exposure a Sn 4d chemical shift of 0.7 eV between the Sn^{4+} and Sn^{2+} components of the Sn 4d core level was identified, equal to the value of the Sn 3d core level shift found by Themlin *et al* [4].

It is well known that the sensing properties of SnO_2 can be improved by doping with a transition metal, but the reaction mechanism of such systems is still not well understood. The gas sensing properties of Pd ultra-thin films deposited either

[5] Author to whom any correspondence should be addressed.

on pyrolytically prepared SnO_x substrates or on SnO_2 powder were studied by XPS and SSIMS [5, 6]. Reversible oxidation and reduction of the Pd additive during heating in air and in hydrogen-enriched air were demonstrated. Pd particles on SnO_2 were easier to oxidize and more difficult to reduce compared to a Pd(111) single crystal. This discrepancy was explained by the different morphology of the systems and by the influence of the interaction between Pd particles and the SnO_2 substrate.

Oxidation reactions induced by exposing the surface to molecular oxygen have been extensively studied for numerous Sn-containing bimetallic compounds. All systems studied so far, including Pd_3Sn [7] and Pt_3Sn [8, 9] bulk alloys, Sn/Pd(111) [10] and Sn/Pt(111) [11] surface alloys, do not oxidize at low O_2 exposures in UHV at 300 K. To achieve oxidation, a high O_2 dose and/or an elevated sample temperature is necessary. An alternative way to oxidize the Sn–transition metal bimetallic compounds is to use more efficient oxidants, such as NO_2 [12, 13] or O_3 [14].

O_2 interaction with a bulk polycrystalline Pd_3Sn alloy surface at elevated temperatures was reported in [7]. Two oxidized Sn states were identified, a quasimetallic PdSnO state resembling an Sn–O chemisorbed state and an Sn oxide state with Sn $3d_{5/2}$ core level shifts of 0.3 and 1.7 eV with respect to the binding energy of the Pd_3Sn alloyed phase. It was shown that, because of low surface Sn mobility, the formation of the two-dimensional oxide is inhibited in favour of the quasimetallic state at temperatures lower than 520 K.

A very limited number of model studies of the Pd–Sn bimetallic system have been performed on single crystals. CO oxidation over a c(2 × 2)-Sn/Pd(100) surface alloy was explored [15] and this surface alloy displays enhancement of CO oxidation rates with lower activation energy compared to the Pd(100) surface. It was concluded that the reaction proceeds at a surface consisting of a disordered SnO_x (x = 1–2) layer on top of the Pd(100) crystal.

More detailed studies were reported by Lee *et al* [10, 16, 17]. In [16] catalytic properties of silica-supported particles (with stoichiometry Pd_2Sn and Pd_3Sn_2) for the conversion of ethyne to benzene and n-hexane were studied. The catalysts were found to be more active than pure Pd, and it was shown that the particles' stoichiometry is strictly related to the selectivity. This work complemented two model studies concerning Sn interaction with a Pd(111) single crystal [17] and the oxidation of the Sn/Pd(111) system [10]. The oxidation of 0.4 and 3.4 ML Sn films prepared by tin deposition on the Pd(111) surface at 300 K has been studied by AES and XPS [10]. The analyses of O 1s photoelectron and O KLL Auger signals for both films showed that oxygen uptake was undetectable below a dose of 10 L O_2. On the 0.4 ML Sn/Pd(111) surface, oxygen adsorption proceeds slowly for exposures up to 10^5 L followed by rapid oxidation at higher exposures, contrary to the 3.4 ML Sn/Pd(111) phase where the tin oxide grows rapidly at low exposures, attaining 90% of the maximum value after 10^5 L O_2 exposure. It was shown that the high pressure oxidation of the Sn thin films at 300 K results in SnO formation for both Sn/Pd(111) phases, in the absence of intermediate or higher oxides. The Sn 3d core level was fitted by two components corresponding to Sn^0 and Sn^{2+} chemical states with 1 eV difference in binding energy, whereas the latter became visible in the spectra only after 1000 L O_2 exposure. It was shown that oxidation of metallic Sn overlayers on the Pd(111) surface eliminates the strong electronic interaction between interfacial Pd and Sn atoms [10].

The oxidation of Sn overlayers on Pt(111) is of relevance to our study, because the Sn/Pt system behaves much like Sn/Pd with respect to the formation of stable surface alloys. Ordered (2 × 2) and ($\sqrt{3} \times \sqrt{3}$)R30° Sn–Pt(111) surface alloys were oxidized by NO_2 exposure at 400 K in UHV [12, 13]. The formation of an interface layer with Sn atoms in the PtSnO quasimetallic state was observed for both oxidized surface alloys. Differences in the amount of sub-surface tin and its segregation to the surface are proposed to explain the higher thermal stability of the oxide overlayer on the ($\sqrt{3} \times \sqrt{3}$)R30° Sn/Pt(111) surface with respect to the oxidized (2 × 2) Sn/Pt(111) surface alloy. The following Sn 3d core level binding energy shifts were reported: 0.4 eV for quasimetallic Pt–Sn–O and 1.4 eV for Sn^{4+} phases with respect to the value for the Sn/Pt(111) surface alloy. For high pressure O_2 oxidation (2.6×10^{-2} mbar at 380–425 K) of these surfaces the same conclusion was drawn with similar binding energy shifts for the quasimetallic and oxidized Sn 3d core level components [11]. High O_2 exposure (>5000 L) at elevated temperatures (>750 K) of the Pt_3Sn (111) and (110) bulk alloy surfaces resulted in the formation of the Sn–O phase with chemisorbed oxygen on the surface. No Sn oxide formation was reported for these surfaces [8, 9].

Although the oxidation of tin has been the subject of numerous investigations, a clear understanding of the process has not yet been achieved. Whether the tin is oxidized at low oxygen exposures at 300 K, and whether the Sn core level binding energy shifts of the oxidized component depend on the tin physical state (bulk sample, thin layer, alloys with other metals, its surface structure and orientation) is not known. In order to gain insight into the mechanisms of Sn oxide formation and into the role of Pd–Sn alloying we have studied the low pressure O_2 oxidation of ordered Sn/Pd(110) surface alloys. The main goal was to investigate the effect of the O_2 exposure on the electronic structure of the Sn/Pd(110) surface alloy by photoelectron spectroscopy using synchrotron radiation.

The present study is motivated by our recent research on Sn–Pd well-defined bimetallic surfaces on Pd(110) [18]. For Sn deposition onto a surface at 300 K, two surface reconstructions were observed: c(2 × 2) and (3 × 1), corresponding to 0.5 and 0.7 ML of Sn coverage. The bimetallic Pd–Sn system is characterized by a strong interaction between Pd and Sn through the hybridization of the Pd d and Sn sp orbitals, leading to the formation of Pd–Sn alloys of noble-metal-like electronic structure. It was shown that, at coverages higher than 0.7 ML, tin is alloyed with the Pd crystal, forming a sub-surface layer of Pd–Sn intermetallic compound whose stoichiometry varies with tin coverage.

2. Experimental details

The experiments were performed at the Materials Science Beamline at the Elettra synchrotron light source in Trieste. The UHV experimental chamber, with a base pressure of 1×10^{-10} mbar, was equipped with a hemispherical electron energy analyser, rear view LEED optics, Sn evaporation source, gas inlet system and an ion gun.

The core level spectra were recorded at normal emission of the photoelectrons with respect to the surface. The photoemission spectra were taken at photon energies 60 and 130 eV for the valence band and Sn 4d core levels (130 eV corresponds to the Cooper minimum of the Pd 4d photoionization cross section; in our previous work [18] we found out that, for the Sn/Pd(110) system, 60 eV is more surface-sensitive than 130 eV), 405 eV for the Pd 3d levels and 600 eV for the O 1s and Sn 3d core levels. The total resolution was determined by measuring the width of the Fermi level at a temperature of 300 K, which gave the following values (photon energy in brackets): 150 meV (60 eV), 130 meV (130 eV), 270 meV (405 eV) and 400 meV (600 eV). The photoelectron peak intensities were normalized to the incident photon flux. Core levels of Sn were fitted by a convolution of a Gaussian and a Doniach–Šunjić line shape with subtraction of a Shirley-type background.

The palladium crystal was a disc of 10 mm diameter and 2 mm thickness, oriented to within 0.1° of the (110) plane. The cleaning procedure consisted of several cycles of sputtering, heating in oxygen and flashing to 870 K. The Sn metal was evaporated from a Knudsen cell onto the clean Pd(110) surface.

The O_2 gas was introduced into the UHV chamber by a leak valve. The O_2 pressures were in the range of 1×10^{-8} to 1.3×10^{-6} mbar during exposures, which are given in Langmuirs ($1\ \text{L} = 1.3 \times 10^{-6}$ mbar s). Oxygen adsorption was performed with the Sn/Pd(110) surface at 300 K.

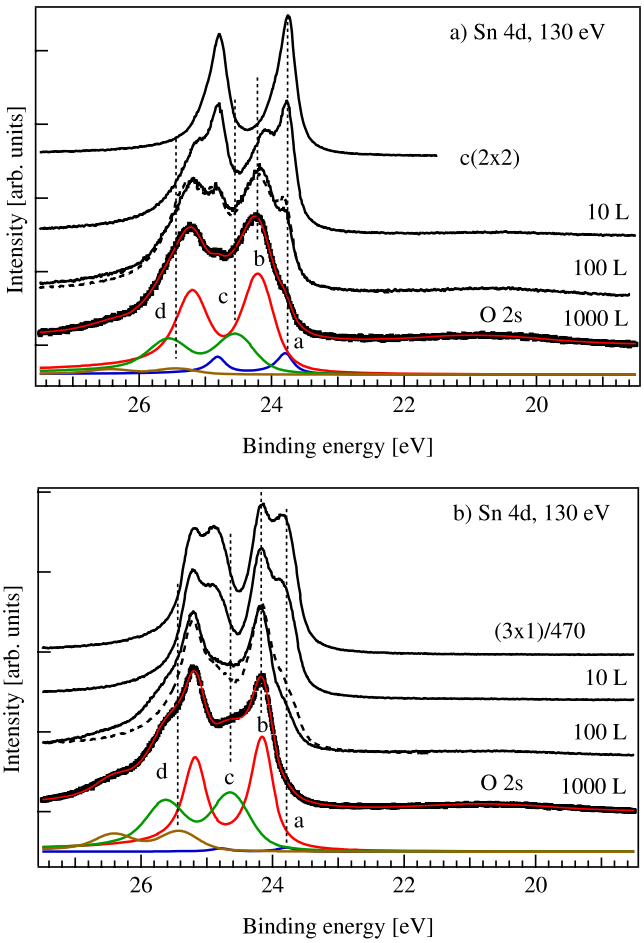

Figure 1. Sn 4d core level spectra before and after O_2 exposure of the (a) c(2 × 2) and (b) (3 × 1)/470 Sn/Pd(110) surface alloy, measured at 130 eV photon energy. Examples of Sn 4d core level fitting are shown for both 1000 L O_2 exposed phases. The dashed line spectra for 100 L dosed surfaces correspond to oxygen adsorption at 120 K.

3. Results

3.1. Sn 4d, O 2s, O 1s and Sn 3d core levels

The surfaces we examined were c(2 × 2) and (3 × 1) reconstructions of the Sn/Pd(110) surface at 0.5 and 0.7 ML Sn coverage, and also a 1.75 ML Sn overlayer on the Pd(110) surface after flashing to 470 K, which also gives a (3 × 1) ordered surface, but there is a considerable amount of sub-surface tin alloyed with palladium, as described in detail in [18]. For brevity, we will refer to the last sample as the '(3 × 1)/470' surface in the rest of the paper. The Sn coverage calibration procedure developed in our previous work [18] was used to prepare the Sn–Pd(110) surface alloys. After each oxygen exposure (1, 10, 100 and 1000 L) of these surfaces, the Sn 4d, Sn 3d, Pd 3d and O 1s core level peaks and valence band spectra were recorded. Increasing the O_2 dose on each Sn/Pd(110) surface alloy results in a diffuse LEED pattern with only substrate diffraction spots, indicating that Sn atoms are randomly displaced from their original positions after oxygen adsorption.

The Sn 4d core level spectra before and after O_2 exposure of the c(2 × 2) and (3 × 1)/470 Sn/Pd(110) surface alloys, measured at 130 and 60 eV photon energy, are shown in figures 1 and 2. The spectra of the (3 × 1) surface, which are omitted, do not contain any new features except those related to the two present surfaces. Starting with a 10 L dose, prominent changes in the spectra were observed for all Sn/Pd(110) surface alloys. The Sn 4d core levels were fitted with several components in order to distinguish between the Sn atoms in different chemical environments and the Sn 4d fitting parameters of the clean Sn/Pd(110) alloy phases were used [18]. The best fit for the 1000 L dosed surface consists of four doublets (see figures 1 and 2). The spin–orbit splitting and branching ratio were kept constant for all Sn 4d doublet components. The Sn 4d doublet branching ratios were 0.8 and 0.65 for the photon energy of 130 and 60 eV, respectively, compared with the ideal ratio of 0.67. The branching ratio was found by curve fitting of the clean Sn/Pd(110) surface spectra, and then used for the analyses of the oxidized surfaces. The higher value of the ratio at 130 eV is attributed to a possible difference in the cross sections or, more probably, photoelectron diffraction effects. The Lorentzian width was in the range of 0.23–0.27 eV for all components while the Gaussian width was allowed to vary to optimize the fit. The

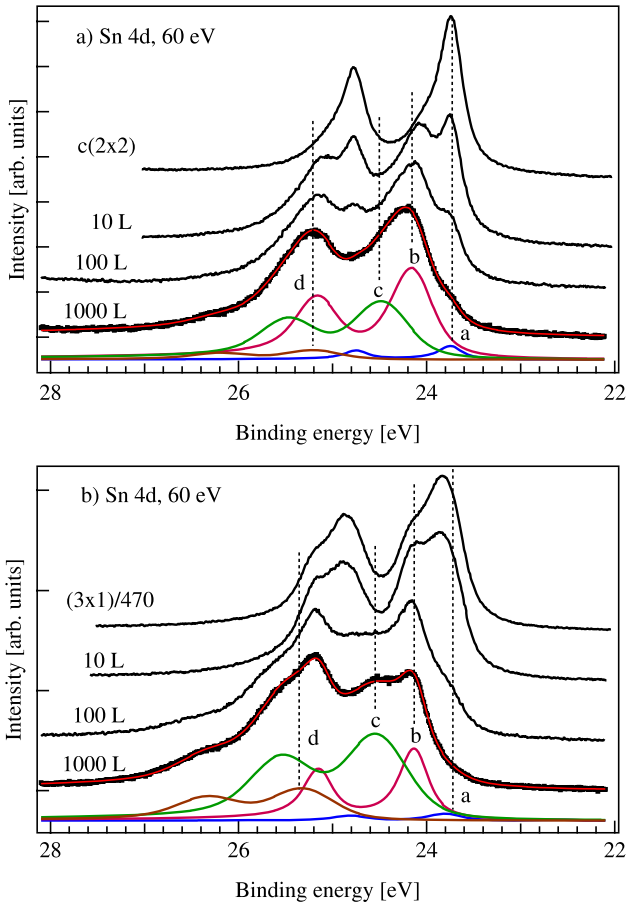

Figure 2. Sn 4d core level spectra before and after O_2 exposure of the (a) c(2 × 2) and (b) (3 × 1)/470 Sn/Pd(110) surface alloy, measured at 60 eV photon energy. Examples of Sn 4d core level fitting are shown for both phases exposed to 1000 L O_2.

Gaussian width of the oxygen-induced Sn 4d components increases from 0.1 to 0.6 eV during oxidation, which is in agreement with the value of 0.5 eV found for tin oxide on polycrystalline Sn foil [3]. The binding energy, Lorentzian and Gaussian widths of the components are listed in table 1 and compared with the values for the oxidized Sn foil [3], which are the only data available in the literature. The Sn 4d components were assigned to Sn atoms in different bonding states: PdSn surface alloy, Pd–Sn–O interface layer or quasimetallic state, SnO and SnO_2 oxide, labelled a, b, c and d in figures 1 and 2, respectively. This assignment will be discussed further below. For the (3 × 1)/470 surface, the high binding energy component of the Sn $4d_{5/2}$ core level, corresponding to the sub-surface Pd–Sn alloy at about 24.1 eV [18], coincides in energy with the Pd–Sn–O component. We did not attempt to fit them separately, so the intensity includes both components.

The Sn 4d core level component intensities together with the Sn 4d total intensity as a function of the O_2 exposure are presented in figure 3. The plots for all surfaces behave very similarly apart from the (3 × 1)/470 surface measured at 60 eV photon energy, for which the Sn^{2+} and Sn^{4+} component signals are higher than the PdSnO one at 1000 L O_2 dose. The ratio of oxide-induced intensities to the total Sn 4d intensity after 1000 L exposure was considered (see table 1, values in brackets). For all considered surfaces the SnO or SnO_2 to PdSnO component ratio is higher for the 60 eV spectra compared to the 130 eV spectra. For the (3 × 1)/470 surface the SnO and SnO_2 relative intensities were 0.52 and 0.19 compared with 0.25 for the PdSnO interface, in the case of the more surface-sensitive spectra measured with a photon energy of 60 eV. The opposite tendency was observed for the 130 eV Sn 4d spectra, where the ratio of the PdSnO to SnO components is in favour of the former. Comparison of the relative intensities of the Sn 4d core level components measured with two photon energies (60 and 130 eV) clearly indicates that the SnO and SnO_2 signal originates from the topmost surface layer, i.e. tin atoms in higher oxidized states constitute the topmost surface layer above the Pd–Sn–O interface.

The O 2s core level has a binding energy of 20.7 eV and is a small, very broad peak on the low binding energy side of the Sn 4d doublet (see figure 1). The O 2s intensity after all O_2 adsorption steps is plotted in figure 4. The O 2s signal growth with dose for the c(2 × 2) and (3 × 1) surfaces is very similar. Different behaviour of the O 2s signal was observed for the (3 × 1)/470 surface, where the adsorption starts at 100 L. This may be due to an autocatalytic effect in which the initial sticking coefficient is very low, but adsorption increases the sticking coefficient, for example by creating active sites. After 10 L O_2 dose, the O 2s intensity ratio for the c(2 × 2) and (3 × 1) surfaces is 0.76, which coincides with the Sn coverage ratio. So we conclude that the amount of adsorbed oxygen is proportional to the Sn coverage for c(2×2) and (3×1) surfaces. At 1000 L dose the oxygen uptake for the (3 × 1)/470 surface is 40% higher than for the other two surfaces.

The O 1s core level overlaps the Pd $3p_{3/2}$ peak, so only the O 1s binding energy and not the intensity was analysed (figure 5). The c(2 × 2) and (3 × 1) Sn/Pd(110) surfaces after 1000 L adsorption are characterized by an O 1s core level binding energy of 529.1 eV. For the (3 × 1)/470 surface, a small O 1s peak shift of 0.3 eV to higher binding energy was observed together with the appearance of a shoulder centred at 531.2 eV. Taking into account the relative intensities of the oxidized Sn 4d core level components (see table 1), it turns out that the topmost layer of the c(2 × 2) and (3 × 1) surfaces is dominated by PdSnO + SnO for which the O 1s peak centroid was found at 529.1 eV. For the oxidized (3 × 1)/470 surface, the binding energy of 529.4 eV was attributed also to the (PdSnO + SnO) phase, and the shoulder at 531.2 eV to the SnO_2 oxide, which is in good agreement with the reference binding energy value for SnO_2 [19]. The binding energy difference of 0.3 eV can be explained by the different relative concentrations of the components which contribute to the (PdSnO + SnO) phase. The measured O 1s binding energy values for the oxidized Sn/Pd(110) surfaces agree rather well with the published data for related systems (see table 2).

For the Sn $3d_{5/2}$ core level, a two-component peak (shifted to higher binding energy with respect to the value of the clean Pd–Sn alloy phase) was observed after 1000 L oxygen exposure (for instance, see figure 6). For quantitative analysis of the Sn $3d_{5/2}$ peak, the fitting parameters of the Sn/Pd(110) surface before oxidation were used for both components. The binding energy values of the components were the same for

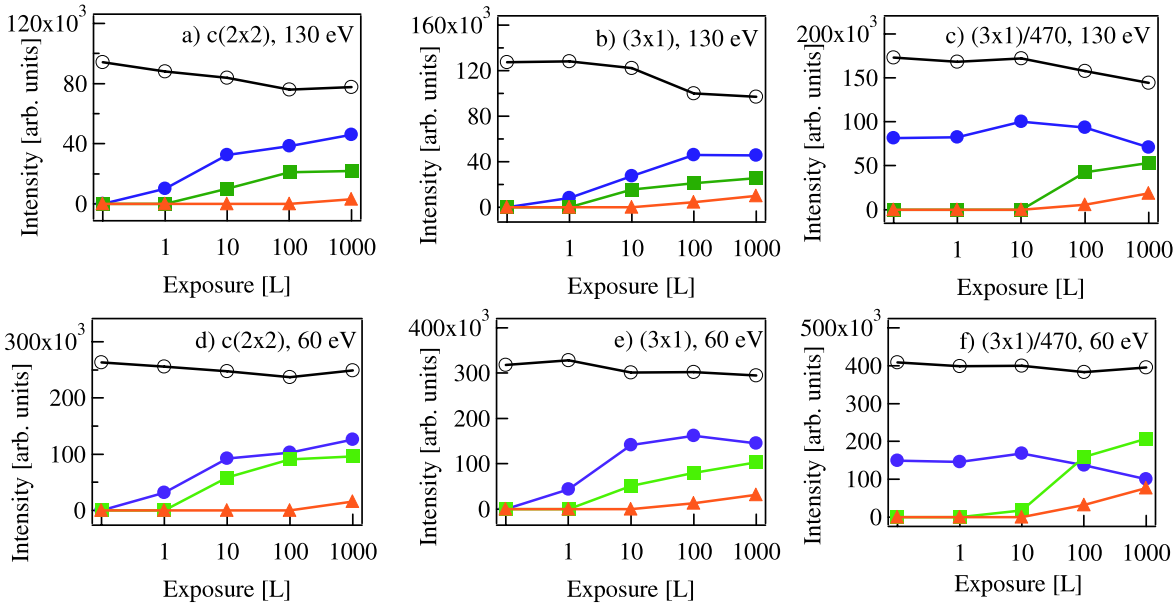

Figure 3. The intensities of the Sn 4d doublets (filled circles—PdSnO (b in figures 1 and 2), filled squares—SnO (c), filled triangles— SnO_2 (d), open circles—total Sn 4d intensity) as a function of O_2 exposure for the c(2 × 2), (3 × 1) and (3 × 1)/470 Sn/Pd(110) surface alloys, measured at 130 and 60 eV photon energies. The estimated error in intensity is 10%.

Table 1. Binding energies, Lorentzian and Gaussian widths (in eV) of the Sn $4d_{5/2}$ core level components labelled a, b, c and d in figures 1 and 2. The value in brackets is the relative intensity with respect to the total Sn $4d_{5/2}$ intensity after 1000 L O_2 exposure. The data for the oxidized Sn foil from [3] are shown for comparison. The binding energy error is less than 0.05 eV.

Sn $4d_{5/2}$	Reference	Sn or $PdSn_{surf}$ (a)	PdSnO (b)	SnO (c)	SnO_2 (d)
O_2/c(2 × 2), 130 eV	This work	23.76 Lw 0.23 Gw 0.09 (0.09)	24.13 Lw 0.27 Gw 0.36 (0.59)	24.44 Lw 0.27 Gw 0.50 (0.28)	25.40 Lw 0.27 Gw 0.51 (0.04)
O_2/c(2 × 2), 60 eV	This work	23.73 Lw 0.24 Gw 0.09 (0.06)	24.10 Lw 0.27 Gw 0.34 (0.50)	24.37 Lw 0.27 Gw 0.50 (0.38)	25.18 Lw 0.27 Gw 0.50 (0.06)
O_2/(3 × 1), 130 eV	This work	23.76 Lw 0.24 Gw 0.11 (0.17)	24.15 Lw 0.27 Gw 0.38 (0.47)	24.52 Lw 0.27 Gw 0.50 (0.26)	25.36 Lw 0.27 Gw 0.50 (0.10)
O_2/(3 × 1), 60 eV	This work	23.74 Lw 0.24 Gw 0.17 (0.05)	24.07 Lw 0.27 Gw 0.36 (0.49)	24.49 Lw 0.27 Gw 0.50 (0.35)	25.25 Lw 0.27 Gw 0.50 (0.11)
O_2/(3 × 1)/470, 130 eV	This work	23.78 Lw 0.24 Gw 0.11 (0.01)	24.16 Lw 0.27 Gw 0.20 (0.49)	24.60 Lw 0.27 Gw 0.50 (0.37)	25.38 Lw 0.27 Gw 0.50 (0.13)
O_2/(3 × 1)/470, 60 eV	This work	23.79 Lw 0.24 Gw 0.26 (0.04)	24.14 Lw 0.27 Gw 0.16 (0.25)	24.60 Lw 0.27 Gw 0.60 (0.52)	25.32 Lw 0.27 Gw 0.60 (0.19)
O_2/Sn foil	[3]	24.0	—	26.6	27.3

all surfaces within experimental uncertainties (see table 3). The clean surface alloys are characterized by an Sn $3d_{5/2}$ core level binding energy of 484.8 eV. For the oxidized Sn/Pd(110) surfaces the dominant peak at 485 eV was assigned to the Pd–Sn–O interface layer and the small peak at 486 eV to the tin oxide. Evidently, we are not able to clearly resolve the SnO and SnO_2 oxide contributions to the high binding energy component of the Sn $3d_{5/2}$ core level because of the low concentration of Sn^{4+} together with the limited experimental resolution.

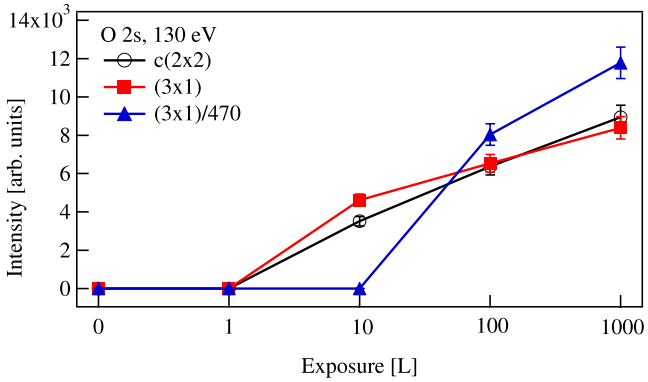

Figure 4. O 2s peak intensity as a function of O_2 exposure for different Sn/Pd(110) surface alloys. The error in the O 2s intensity is below 5%.

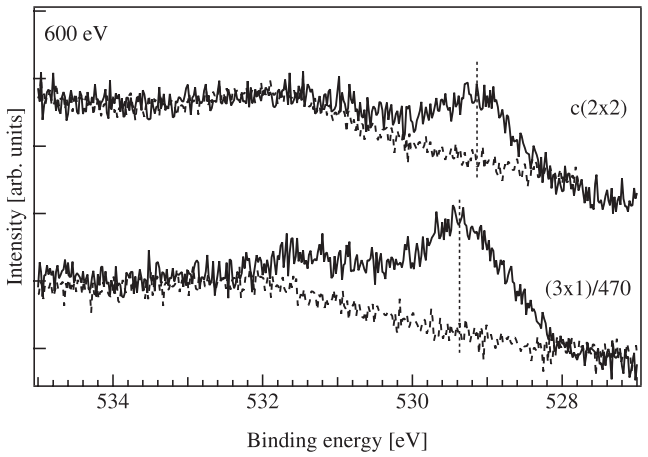

Figure 5. The Pd $3p_{3/2}$ and O 1s core levels for the c(2 × 2) and (3 × 1)/470 phases after 1000 L O_2 exposure (solid line) compared with clean surface spectra representing the Pd $3p_{3/2}$ states (dashed line).

3.2. Valence band and Pd 3d core level spectra

The change of the valence band spectra after O_2 adsorption on the c(2 × 2) and (3 × 1)/470 Sn/Pd(110) surface alloys, measured at 130 and 60 eV photon energies, are shown in figures 7 and 8. The data acquired on the (3 × 1) surface are again not shown since the behaviour was similar to the c(2 × 2) one. With increasing O_2 dose, the spectra acquired with 130 eV light contain a new peak at a binding energy of 4.4 eV for all surfaces, which was assigned to O 2p derived states. The O 2p intensity increases gradually for the c(2 × 2) phase while it rises sharply after 100 L dose for the (3 × 1)/470 surface, in agreement with the O 2s signal behaviour (figure 4). We conclude that the presence of the sub-surface alloy layer is responsible for increased oxygen adsorption on the Sn/Pd(110) surface alloys. The shoulder at about 9 eV was attributed to CO molecular adsorption (4σ CO molecular orbital [18]) from the residual gases in vacuum; at this photon energy, photoemission is extremely sensitive to this adsorbate. Because of the low cross section and low surface concentration of tin atoms, we did not observe the characteristic feature for SnO oxide in the valence band spectra at 2 eV [4].

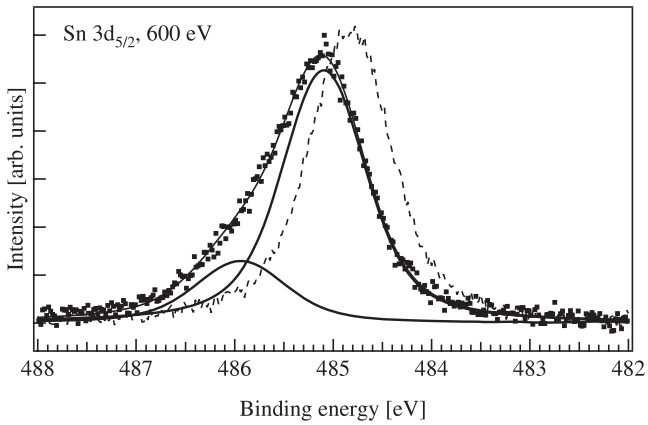

Figure 6. The Sn $3d_{5/2}$ core level for the (3 × 1)/470 Sn/Pd(110) phase after 1000 L O_2 exposure (dots) with corresponding fitted components, measured at 600 eV photon energy. The clean (3 × 1)/470 phase spectrum is shown for comparison (dashed line).

Table 2. O 1s core level binding energies (in eV) for the Sn/Pd(110) surfaces after 1000 L O_2 exposure, and comparison with published data for related systems. 'M' indicates metal, either Pd or Pt.

O 1s	Reference	MSnO	SnO	SnO_2
O_2/c(2 × 2) Sn/Pd(110)	This work	529.1		—
O_2/(3 × 1) Sn/Pd(110)	This work	529.1		—
O_2/(3 × 1)/470 Sn/Pd(110)	This work	529.4		531.2
O_2/Pd_3Sn	[7]	529.5	530.4	
O_2/Sn/Pd(111)	[10]	—	529	—
O_2/Sn/Pt(111)	[11]	529.7		
NO_2/Sn/Pt(111)	[12]	528.8	—	529.9
SnO	[20]	—	530.4	—
SnO_2	[19]	—	—	531.4

In the valence band spectra at 130 eV, bands with maxima at 1.6 eV for the c(2 × 2) surface and 1.9 eV for the (3 × 1)/470 surface were only slightly influenced by O_2 adsorption, i.e. they became less resolved and formed a low binding energy shoulder of the O 2p derived peak (figure 7). Contrary to this, in the 60 eV spectra the position of bands at 1.25 eV for the c(2 × 2) surface and at 1.9 eV for the (3 × 1)/470 surface shifts with increasing oxygen uptake (figure 8). Moreover these shifts are in different directions: an increase from 1.25 to 1.4 eV for c(2 × 2) and a decrease from 1.9 eV to 1.65 eV for the (3 × 1)/470 surface. As we have shown in our previous paper [18], these two bands are characteristic of the Sn/Pd(110) surface alloy phases, the band maxima of which shift to higher binding energy with increasing amounts of adsorbed tin. For the c(2 × 2) surface, the shift of the 1.25 eV band to higher binding energy is in agreement with the general tendency for the core level and valence band spectra of metals on oxidation. For the (3 × 1)/470 surface, the shift of the 1.9 eV band to lower binding energy was attributed to a change in the Sn/Pd(110) surface alloy composition caused by the oxygen adsorption. Evidently the stoichiometry of Pd–Sn intermetallic compounds was altered after O_2 adsorption. We suggest that the Sn–O bond formation is accompanied by Pd–Sn bond dissociation, as was observed in the case of the Sn/Pd(111) system [10]. In other words the amount of tin dissolved in the Pd crystal is reduced by segregation of tin to

Table 3. Binding energies (in eV) of the Sn $3d_{5/2}$ core level and comparison with published data for related systems. The values in brackets are the relative intensity of the peak component with respect to the total Sn $3d_{5/2}$ intensity after 1000 L O_2 adsorption. 'M' indicates metal, either Pd or Pt.

Sn $3d_{5/2}$	Reference	Sn or MSn before O_2	MSnO	SnO	SnO_2
O_2/c(2 × 2) Sn/Pd(110)	This work	484.7	485.0 (0.95)	485.9 (0.05)	
O_2/(3 × 1) Sn/Pd(110)	This work	484.8	485.1 (0.85)	486.0 (0.15)	
O_2/(3 × 1)/470 Sn/Pd(110)	This work	484.8	485.1 (0.79)	485.9 (0.21)	
SnO, SnO_2	[4]	483.8	—	485.6	486.3
O_2/Pd_3Sn	[7]	483.3	483.6	485	
O_2/0.4 ML Sn/Pd(111)	[10]	484.5	—	485.3	—
O_2 /3.4 ML Sn/Pd(111)	[10]	484.1	—	485.0	—
O_2/(2 × 2), ($\sqrt{3} \times \sqrt{3}$)R30° Sn/Pt(111)	[11]	484.9	485.5	486.3 SnO_x, $x < 2$	
NO_2/($\sqrt{3} \times \sqrt{3}$)R30° Sn/Pt(111)	[12]	484.6	485.0	—	486.0
SnO	[20]	—	—	486.5	—
SnO_2	[19]	—	—	—	487.5

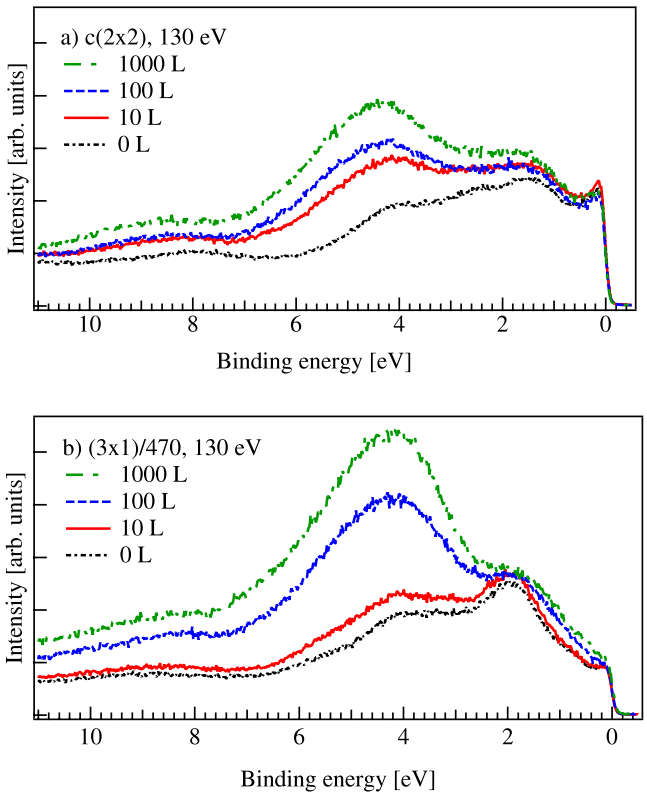

Figure 7. Valence band spectra before and after O_2 exposure of the (a) c(2 × 2) and (b) (3 × 1)/470 Sn/Pd(110) surface alloy, measured at 130 eV photon energy.

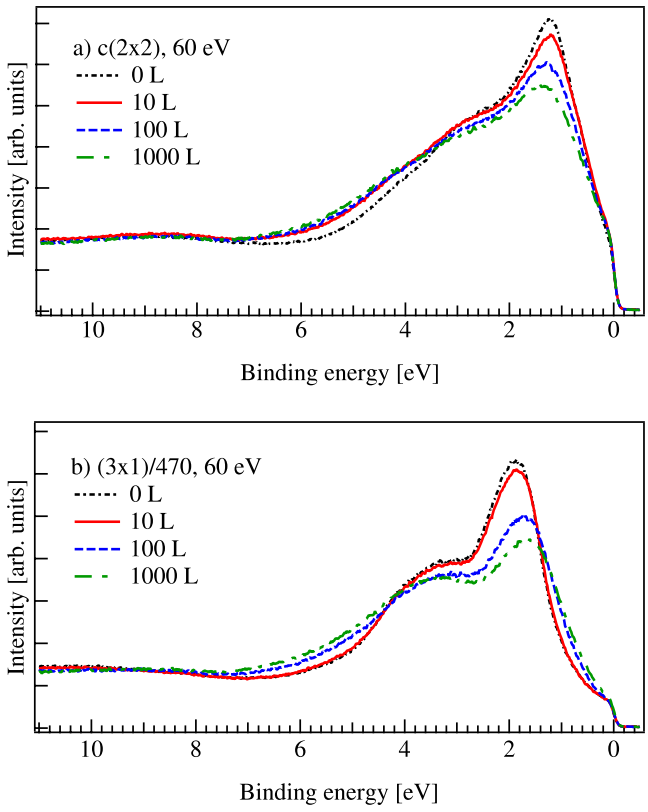

Figure 8. Valence band spectra before and after O_2 exposure of the (a) c(2 × 2) and (b) (3 × 1)/470 Sn/Pd(110) surface alloy, measured at 60 eV photon energy.

the surface to form the tin oxide overlayer. The valence band maxima shifts observed in the more surface-sensitive spectra (measured at 60 eV photon energy) indicate that the Pd–Sn alloy composition change takes place mainly at the surface, influencing the stoichiometry of the sub-surface intermetallic compounds. The increase of the density of state in the region from 1.4 to 0.4 eV after O_2 adsorption, visible in the spectra measured at both photon energies, was also attributed to the fact that the surface tin oxidation affects the sub-surface tin layers and, as a result, we obtained a more Pd-rich Pd–Sn sub-surface alloy layer.

The latter conclusion was also confirmed by the Pd $3d_{5/2}$ core level behaviour (figure 9). Apart from the intensity change, the Pd 3d core level was only slightly influenced

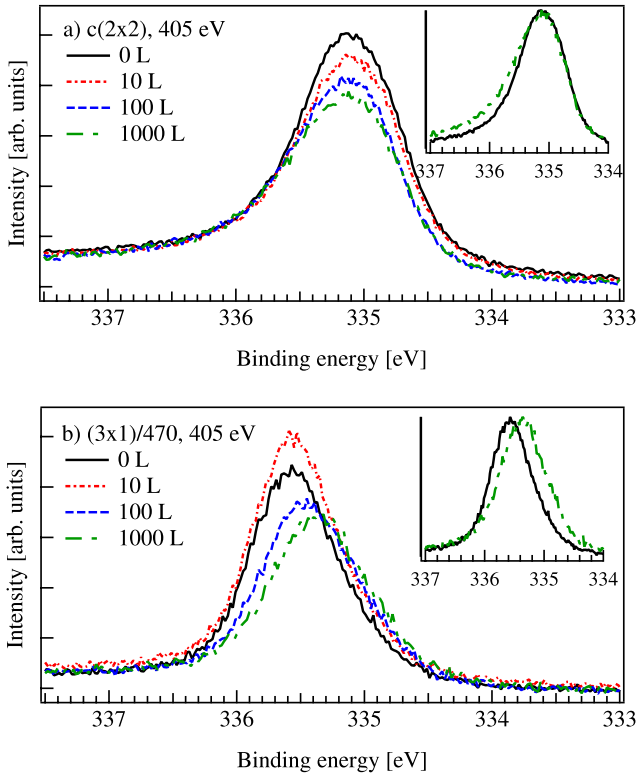

Figure 9. Pd $3d_{5/2}$ core level spectra for the (a) c(2 × 2) and (b) (3 × 1)/470 phases before and after oxygen exposure, measured at 405 eV photon energy. The insets show the Pd $3d_{5/2}$ spectra normalized to one another for the clean and 1000 L O_2 exposed phases.

by the adsorption of oxygen on the c(2 × 2) surface. The intensity increase at about 336 eV binding energy was detected as a result of the oxygen uptake, which was attributed to PdSnO bond formation (see the inset in figure 9(a)). In the case of the (3 × 1)/470 surface, the Pd $3d_{5/2}$ core level shifts to lower binding energy from 335.6 to 335.35 eV after 1000 L O_2 adsorption (see the inset of figure 9(b)). The peak remains symmetric at the binding energy of 335.35 eV, which is higher than the value for bulk Pd [18]. We conclude that the Pd 3d core level corresponds to the Pd–Sn alloy phase, the stoichiometry of which was changed by oxygen adsorption. As a result a Pd–Sn sub-surface alloy with higher concentration of Pd is formed. This interpretation is consistent with the earlier conclusions on the Sn–O bond formation at the cost of Pd–Sn dissociation for surfaces with the sub-surface Pd–Sn intermetallic layer.

4. Discussion

We propose the same oxidation mechanism for Sn/Pd(110) surface alloys as was reported for the Sn/Pt(111) and Pd_3Sn systems oxidized at high O_2 pressures [7, 11]. Oxygen dissociatively chemisorbs on the alloy surface and either diffuses to or adsorbs directly at the nearest Sn atom, which strongly interacts with oxygen. Then oxygen adsorption on the Sn atoms alloyed with Pd only slightly influences the intermetallic bond. When an excess of oxygen is present, i.e. when the PdSnO saturation coverage is reached, formation of SnO and SnO_2 occurs with an SnO_2 overlayer emerging at high O_2 exposures.

The Sn 4d core level binding energy is very sensitive to the oxidation state change of tin. For all surfaces the Sn 4d core level was fitted by an (inter) metallic Sn component plus three oxygen-induced Sn^{x+} components with binding energies of about 24.12, 24.5 and 25.3 eV, which were associated with PdSnO, Sn^{2+} and Sn^{4+} species, respectively. While the Sn 4d core level is strongly affected by O_2 adsorption, the Sn 3d core level showed only a small shift from 484.7 to 485.0 eV, with a small second component peak at 486 eV binding energy, because of low resolution at 600 eV photon energy.

For the c(2 × 2) and (3 × 1) Sn/Pd(110) surfaces, the oxygen content in the surface layer increases monotonically from the first adsorption, mainly due to formation of the PdSnO phase, with about 35% of tin present as Sn^{2+} after 1000 L O_2 adsorption. Most likely the oxide layer is not continuous for these surfaces because of the limited amount of tin in the surface, 0.5 ML for c(2 × 2) and 0.7 ML for (3 × 1) surface. Contrary to the previous two surfaces, O_2 adsorption on the (3 × 1)/470 Sn/Pd(110) surface alloy results in progressive accumulation of oxygen in the surface starting with the 100 L O_2 dose. After the highest exposure, mainly Sn^{2+} and Sn^{4+} atoms were found as dominating species on the surface with only 25% in the PdSnO phase. As in the cases of Sn/Pd(111) [10] and Sn/Pt(111) [11], we can conclude that the tin oxide film wets the bimetallic surface, i.e. the surface free energy of the oxide is lower than that of the Sn/Pd(110) surface. The total Sn 4d intensity did not change for the (3 × 1)/470 Sn/Pd(110) surface, and only redistribution of tin within the surface and sub-surface layers was observed. The presence of the sub-surface alloy layer has a key role in the oxygen uptake mechanism on the Sn/Pd(110) surface alloys. Apparently the oxidation is kinetically controlled, i.e. Sn segregation into the surface region allowed for tin oxide growth, and was accompanied by Pd–Sn intermetallic bond breaking. Oxygen adsorption on the Sn/Pd(110) surface, which comprises extraction of alloyed Sn atoms to form a tin oxide overlayer, has also been reported in oxidation studies of Sn/Pd(111), Sn/Pt(111) and Pd_3Sn systems [7, 10, 11].

The results of the present study are in contrast with those published for the Sn/Pd(111) system where sub-monolayer Sn coverages were stable towards an O_2 exposure of less than 1000 L [10]. There are two possible reasons for this difference: (1) the different orientation of the palladium substrates, i.e. Pd–Sn intermetallic compounds on the more open Pd(110) surface more readily adsorb oxygen, and (2) the weak interaction of the Sn overlayer with the Pd(111) surface at 300 K [10] for which the effect of the intermetallic bond on the interaction with oxygen is minimized.

Our results agree well with those for tin metal oxidation, where first SnO appears, which in the presence of excess oxygen oxidizes to SnO_2. On O_2 adsorption, the PdSnO quasimetallic states we found for Sn/Pd(110) alloy surfaces are not present for clean Sn metal and are a new feature of the Pd–Sn 2D surface alloy. No change of the Sn 4d core level up to 200 L O_2 exposure at 300 K was observed for tin foils [3]. We

have shown that the presence of the Sn–Pd intermetallic bonds facilitates tin oxide formation on Pd(110), where the oxygen adsorption starts from a dose of 10 L.

Similar results were obtained on O_2 exposure of the studied surfaces at 120 K (for instance, see the dashed spectra in figure 1). For c(2 × 2) and (3 × 1) surfaces there are almost no differences in the Sn 4d spectra after 100 L O_2 dose. We suggest that, for Pd–Sn surface alloys in the absence of sub-surface tin, the oxidation process is limited only by the sticking coefficient of oxygen, and not by surface diffusion. The Sn 4d spectra of the (3 × 1)/470 Sn/Pd(110) surface after 100 L O_2 adsorption at 300 K and 120 K are different: the Sn^{2+} and Sn^{4+} components of the Sn 4d spectrum are lower, while Sn^0 is higher. This confirms the conclusion that Sn segregation into the surface region contributes to efficient tin oxide growth.

5. Conclusions

Three Pd–Sn surface alloys have been examined by photoelectron spectroscopy after exposure to oxygen at 300 K and low pressure: the ordered c(2 × 2) and (3 × 1) surface structures with tin atoms located only in the top layer, and the (3 × 1) one with the sub-surface Pd–Sn layer (labelled (3 × 1)/470). Exposure of these alloys to oxygen results in an LEED pattern with diffuse substrate spots and the c(2 × 2) and (3 × 1) spots disappeared. No additional superstructure was observed.

Three oxygen-induced Sn states were found by fitting the Sn 4d doublet: the PdSnO chemisorbed state, and two oxides, SnO and SnO_2. The Pd 3d core level and valence band spectra analysis confirms the assignment. The PdSnO quasimetallic state was found to be a characteristic feature for Pd–Sn surface alloys. It was shown that the SnO or SnO_2 oxides constitute the topmost surface layer on top of the Pd–Sn–O interface. O_2 adsorption on the (3 × 1)/470 Sn/Pd(110) surface was shown to result in progressive accumulation of oxygen in the surface, which is controlled by Sn diffusion and accompanied by Pd–Sn intermetallic bond dissociation. It was concluded that the presence of a sub-surface Pd–Sn intermetallic alloy facilitates the tin oxide formation.

Acknowledgments

NT acknowledges the support of the Japan Society for the Promotion of Science. The Materials Science Beamline is supported by the Ministry of Education of the Czech Republic under grant no. LC06058. We thank our colleagues at Elettra for their help and assistance.

References

[1] Batzill M and Diebold U 2005 *Prog. Surf. Sci.* **79** 47
[2] Batzill M, Katsiev K, Burst J M, Losovyj Y, Bergermayer W, Tanaka I and Diebold U 2006 *J. Phys. Chem. Solids* **67** 1923
[3] De Padova P, Fanfoni M, Larciprete R, Mangiantini M, Priori S and Perfetti P 1994 *Surf. Sci.* **313** 379
[4] Themlin J M, Chtaib M, Henrard L, Lambin P, Darville J and Gilles J M 1992 *Phys. Rev.* B **46** 2460
[5] Skála T, Veltruská K, Moroseac M, Matolínová I, Cirera A and Matolín V 2004 *Surf. Sci.* **566–568** 1217
[6] Moroseac M, Skála T, Veltruská K, Matolín V and Matolínová I 2004 *Surf. Sci.* **566–568** 1118
[7] Rotermund H H, Penka V, De Louise L A and Brundle C R 1987 *J. Vac. Sci. Technol.* A **5** 1198
[8] Hoheisel M, Speller S, Heiland W, Atrei A, Bardi U and Rovida G 2002 *Phys. Rev.* B **66** 165416
[9] Hoheisel M, Speller S, Atrei A, Bardi U and Rovida G 2005 *Phys. Rev.* B **71** 35410
[10] Lee A F and Lambert R M 1998 *Phys. Rev.* B **58** 4156
[11] Jerdev D I and Koel B E 2001 *Surf. Sci.* **492** 106
[12] Batzill M, Beck D E, Jerdev D and Koel B E 2001 *J. Vac. Sci. Technol.* A **19** 1953
[13] Batzill M, Kim J, Beck D E and Koel B E 2004 *Phys. Rev.* B **69** 165403
[14] Saliba N A, Tsai Y L and Koel B E 1999 *J. Phys. Chem.* B **103** 1532
[15] Logan A D and Paffett M T 1992 *J. Catal.* **133** 179
[16] Lee A F, Baddeley C J, Hardacre C, Moggridge G D, Ormerod R M, Lambert R M, Candy J P and Basset J-M 1997 *J. Phys. Chem.* B **101** 2797
[17] Lee A F, Baddeley C J, Tikhov M C and Lambert R M 1997 *Surf. Sci.* **373** 195
[18] Tsud N, Skála T, Šutara F, Veltruská K, Dudr V, Fabík S, Sedláček L, Cháb V, Prince K C and Matolín V 2005 *Surf. Sci.* **595** 138
[19] Jiménez V M, Mejías J A, Espinós J P and González-Elipe A R 1996 *Surf. Sci.* **366** 545
[20] Jiménez V, Fernández A, Espinós J P and González-Elipe A R 1996 *Surf. Sci.* **350** 123